Construction and Building Materials 497 (2025) 143795

Contents lists available at ScienceDirect

Construction and Building Materials

journal homepage: www.elsevier.com/locate/conbuildmat

# Optimization of recycled asphalt binder with eco-friendly additives: Activation energy and bonding properties

Abdul Samad [a], Xue Luo [a], Jiawei Wang [b,*], Muhammad Waheed Abid [a]

[a] College of Civil Engineering and Architecture, Zhejiang University, Hangzhou 310058, China
[b] Department of Chemical Engineering, Swansea University, Bay Campus, Swansea SA1 8EN, UK

ARTICLE INFO

*Keywords:*
Waste material
RAP
Rejuvenators
Kinetic approach
Activation energy
Additives

ABSTRACT

To address the challenges of developing eco-friendly and sustainable asphalt binders, this study explores the use of three primary waste materials from the automobile and pavement industries: crumb rubber (CR), waste engine oil (WEO), and reclaimed asphalt pavement (RAP). While previous studies have explored the use of individual or dual rejuvenators, limited research has examined multiple additives for rejuvenating 100 % RAP binders. This study addresses this gap by evaluating the effect of sequentially adding CR, WEO, and SBS on the aging, cracking, rheological, and bonding properties of laboratory-produced RAP binders. Kinetic modeling (via Arrhenius equations) was employed to quantify aging activation energy ($E_{aa}$), cracking activation energy ($E_{ac}$), and viscous flow activation energy ($E_v$). Four rejuvenated binders were prepared using different contents of additives (6 % CR, 7.5 % and 10 % WEO, and 2 % and 3 % SBS), and their performance was compared to virgin and RAP binders. Results indicate that adding 10 % WEO, 6 % CR, and 3 % SBS improves fatigue resistance, as evidenced by higher cracking activation energy and improved adhesive bond strength. The blend with 7.5 % WEO, 6 % CR, and 3 % SBS demonstrated superior high-temperature performance in multiple stress creep and recovery (MSCR) tests. Notably, the blend with 10 % WEO, 6 % CR, and 2 % SBS exhibited the lowest viscosity among the rejuvenated binders, enhancing workability and flow characteristics. These findings demonstrate the potential of multi-additive blends to improve the durability and sustainability of RAP binders, offering a promising solution for extending pavement service life.

## 1. Introduction

Asphalt pavement, renowned for its cost-effectiveness and durability, plays an important role in economic and societal development. It is widely used in various sectors, especially pavement construction, where asphalt binder is a primary material. Asphalt binder, composed of asphaltenes and maltenes, undergoes oxidative aging, altering its chemical and physical properties. It becomes more viscous and prone to fatigue and low-temperature cracking, with increased asphaltene content leading to pavement distress and the generation of reclaimed asphalt pavement (RAP) [1].

China generates over 200 million tons of RAP each year [2]. Reusing RAP provides a sustainable solution, offering economic benefits while reducing greenhouse gas emissions and energy use [3]. However, the aging of RAP binders leads to increased stiffness and viscosity, decreased surface free energy, and a weakened asphalt-aggregate interface, making RAP more susceptible to early fatigue and moisture damage compared to virgin asphalt [4–6].

To address these issues, petroleum or organic-based rejuvenators are added to RAP (i.e., aged binder), reducing viscosity and improving resistance to low-temperature and fatigue cracking [4,7]. Commercial rejuvenators, mainly derived from oil industry byproducts, are widely used for this purpose. In pursuit of more sustainable alternatives, studies suggest using waste oils like waste engine oil (WEO) and waste cooking oil (WCO) to improve fatigue resistance, low-temperature cracking, and mix workability [8,9]. WEO, a petroleum byproduct that causes environmental issues when improperly disposed of after use, is particularly effective as a rejuvenator by restoring the binder's light fractions, adjusting the asphaltene/resin ratio, and enhancing workability [10–12]. The addition of WEO to RAP binder significantly improves its rheological properties, making it less stiff and more resistant to aging [13]. Another study examined the effects of WEO and WCO on RAP asphalt binders, finding that both oils enhanced penetration, ductility, and workability while improving fatigue performance and lowering the

* Corresponding author.
*E-mail addresses:* abdulsamad@zju.edu.cn (A. Samad), xueluo@zju.edu.cn (X. Luo), jiawei.wang@swansea.ac.uk (J. Wang), dr.mwa@zju.edu.cn (M.W. Abid).

https://doi.org/10.1016/j.conbuildmat.2025.143795
Received 28 November 2024; Received in revised form 2 September 2025; Accepted 26 September 2025
Available online 6 October 2025

softening point and Brookfield viscosity [14]. While these benefits are significant, excessive use of oil-based rejuvenators can negatively affect elastic recovery, rutting resistance, and low-temperature cracking resistance [15].

Another major waste material is tire-derived crumb rubber (CR). With approximately 3.2 million tons of waste tires generated annually, CR presents an opportunity for sustainable asphalt modification [16]. CR, composed of natural and synthetic rubber with sulfur-carbon black cross-links, improves binder recovery, reduces moisture damage, and enhances stiffness and rutting resistance when added to asphalt [16,17]. Studies indicate that effective CR content typically ranges from 5 % to 10 % by weight [18]. On the other hand, CR-modified asphalt binders face challenges such as increased viscosity, incompatibility, reduced stability, and higher mixing and compaction temperatures [18,19]. Styrene-butadiene-styrene (SBS) copolymer is commonly employed in asphalt binders due to its excellent thermal stability and longevity. As a thermoplastic elastomer, SBS enhances elastic recovery, adhesion, cohesion, and resistance to both low-temperature cracking and high-temperature rutting [20,21]. Nevertheless, increased SBS content raises binder viscosity, reduces economic feasibility, and increases production costs [22].

To address the limitations of WEO, CR, and SBS in asphalt binder, researchers have explored combining these materials to optimize performance. For instance, the combination of WEO and re-refined engine oil bottoms (REOB) with polymers, particularly SBS, has been found to enhance rutting resistance, fatigue performance, and flexibility of asphalt binders [22,23]. Additionally, adding bio-oil to SBS-modified asphalt has been shown to improve intermediate and low-temperature performance while slowing the aging process [24]. Studies on WEO and CR addition to asphalt binders suggest that 5 % WEO with 8 % CR improved workability, oxidation resistance, and rutting resistance [20]. Similarly, SBS and CR have been evaluated using Linear Amplitude Sweep (LAS) and Time Sweep (TS) tests to assess fatigue performance. Results indicated that adding CR with SBS significantly increased the fatigue life of the base asphalt [22]. Furthermore, adding CR and SBS to asphalt binders has been shown to influence thermal oxidative aging mechanisms, resulting in superior anti-aging performance compared to their individual addition [25]. In addition, waste oils (WCO and WEO) with styrene-butadiene rubber (SBR) have demonstrated improved fatigue and rutting resistance [26].

Beyond these rejuvenators, other sustainable materials such as polyethylene (PE), waste plastics, waste glass, waste polypropylene (PP), low-density polyethylene (LDPE), and polyethylene terephthalate (PET) have also been explored in pavement applications [27,28]. Despite these advancements, there remains a lack of studies investigating how the combined addition of WEO, CR, and SBS influences aged asphalt performance. Furthermore, limited research has integrated chemical aging indices, kinetic modeling, and fatigue performance evaluation when assessing rejuvenator effectiveness.

Understanding the long-term performance of asphalt binders requires analyzing their behavior across time, temperature variations, and reaction rates. Kinetic modeling plays a crucial role in predicting binder aging, fatigue crack growth, viscous flow behavior, and self-healing properties. Previous studies have effectively used kinetics-based models to analyze these aspects in both base and recycled asphalt binders [29–34].

The Arrhenius framework characterizes the temperature dependence of asphalt binders under the assumption that the activation energy remains constant and the reaction follows fixed-order kinetics over the studied temperature range, with its validity being most appropriate in the linear response region. When the rate constant is physically meaningful and properly formulated, the resulting activation energy can be considered reliable. The temperature susceptibility of asphalt is often influenced by its viscoelastic properties, such as viscosity, complex modulus, and phase angle, which further complicates its characterization. In addition, it depends on binder type, aging condition, modifier type, and viscoelastic parameters applied [35]. Despite these complexities, Arrhenius-based modeling remains a valuable tool, as it enables comparison of different binders, assessment of aging effects, and prediction of temperature-dependent behavior [36]. Investigating the kinetic behavior of asphalt binders is therefore essential for predicting their prolonged performance and enhancing durability, especially regarding fatigue cracking and oxidative aging, which are key failure mechanisms in asphalt pavements [32]. A higher activation energy indicates a greater kinetic barrier, requiring more energy for processes such as cracking, aging, and flow [29,37]. For instance, higher activation energy for crack propagation reflects improved resistance to fatigue cracking, since more energy is required to initiate damage compared to binders with lower activation energies, thereby corresponding to superior fatigue performance [38].

This study examines the combined effects of WEO, CR, and SBS on aged RAP binder performance, addressing the existing research gap in the application of multiple rejuvenators. It highlights the synergistic interactions between these materials, where light components in WEO are absorbed by SBS and CR, leading to improved binder homogeneity and enhanced overall performance, while balancing the limitations associated with their individual use. Unlike previous studies that focus on single or binary rejuvenator systems, this study introduces a multi-additive approach that leverages the complementary properties of WEO, CR, and SBS. Kinetic modeling is employed to evaluate the aging process and fatigue cracking, while rheological and adhesion performance assessments provide insights into the long-term durability. These efforts aim to explore the relationships between activation energy, surface energy characteristics, and rheological properties, ultimately enhancing our understanding of binder rejuvenation and performance optimization.

## 2. Materials & preparation

### 2.1. Materials

The base asphalt binder (70# binder) was artificially aged using a Thin Film Oven (TFO) followed by a Pressure Aging Vessel (PAV). The TFO test, following ASTM D2872–19, was performed on 70# binder at 163 °C for 300 ± 5 min. Subsequently, the TFO-aged asphalt underwent PAV aging according to AASHTO R28–09 at 100 °C for 20 h under 2.1 ± 0.1 MPa [39]. The resulting asphalt, referred to as PAV-aged binder (PB), simulates the characteristics of RAP binder.

The materials used in this study—waste engine oil (WEO), crumb rubber (CR), and styrene-butadiene-styrene (SBS)—were sourced locally from Hangzhou, China, shown in Fig. 1. WEO, a black oily liquid with a viscosity of 93.52 cP (at 60 °C), was collected directly from a local garage. CR, derived from reclaimed waste vehicle tires, had a particle size of 80 mesh (0.178 mm). SBS was a linear-grade copolymer

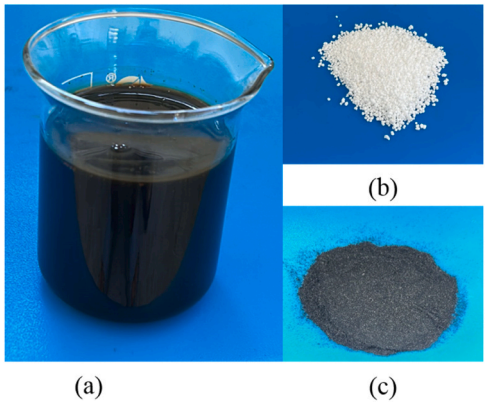


**Fig. 1.** Raw materials: (a) WEO, (b) SBS, (c) CR.

(SBS1301–1, YH-791) with an average molecular weight of approximately 100,000 g/mol and a styrene content of 30 %.

The PB binder was rejuvenated through sequential incorporation of three additives: WEO, (7.5 and 10 %), CR (6 %, No. 80 mesh/0.177 mm), and linear SBS polymers (2 and 3 %), all added by weight of PB. WEO was preheated in an oven at 60 °C and then blended with PB at 150 °C using a shear mixer set at 1000 rpm for 30 min [26]. CR was subsequently added to the WEO-rejuvenated binder, with initial low-speed mixing followed by high-shear blending (3500 rpm, 170–180 °C, 35–45 min) to depolymerize rubber hydrocarbon chains. Finally, SBS was incorporated at 180 °C (4000 rpm, 40 min) to form cross-linked stable networks within CR-WEO-rejuvenated matrix [40,41]. The blend was stored for one day to allow stabilization, then reheated to 160 °C and mixed at 1000 rpm for 30 min to ensure homogeneity and stabilization of polymer–binder interactions prior to testing. Table 1 outlines the rejuvenated binders with varying additive contents.

## 3. Testing

The testing and evaluation methods are illustrated in Fig. 2.

### 3.1. Aging test

Oven aging procedures were conducted to evaluate the oxidative aging reaction kinetics and assess the aging resistance of various binder samples. PAV aging was conducted at various temperatures and durations. To replicate oxidative aging for each asphalt binder, three temperatures (90 °C, 100 °C, and 110 °C) and three durations (10 h, 20 h, and 40 h) were chosen. Asphalt samples of approximately 50 g ± 0.5 g were used for each aging condition.

### 3.2. FTIR test

Fourier Transform Infrared (FTIR) spectroscopy is used to analyze the chemical structure and functional groups, particularly carbonyl groups, in asphalt samples. Thirty-two scans were performed across the 4000 $cm^{-1}$ to 650 $cm^{-1}$ range at a 4 $cm^{-1}$ resolution. Changes over time can be observed, and the aging activation energy ($E_{aa}$) can be determined.

### 3.3. Surface energy test using Wilhelmy Plate (WP)

Surface Free Energy (SFE) was evaluated using the Wilhelmy Plate (WP) technique. In this method, a thin glass plate coated with asphalt is immersed in a liquid, and then slowly withdrawn to measure the contact angle (θ) between the liquid and the asphalt surface [42].

Contact angles were measured using three different probe liquids (Formamide, Glycerol, and distilled water) with known SFE properties at 20 °C. Each type of asphalt was tested in parallel in triplicate for each liquid. The SFE components of the binders and liquids were calculated using the Young-Dupre equation, shown in Eq. (1) [43].

$$\left(1+\cos\theta\right)\gamma_L = 2\left(\sqrt{\gamma_S^{LW}\gamma_L^{LW}} + \sqrt{\gamma_S^{+}\gamma_L^{-}} + \sqrt{\gamma_S^{-}\gamma_L^{+}}\right) \quad (1)$$

Where $\gamma_S^{LW}$ and $\gamma_L^{LW}$ are the Lifshitz-van der Waals components of asphalt binder and the liquid, respectively; $\gamma_S^{+}$ and $\gamma_L^{+}$ are the Lewis acid components of the asphalt binder and the liquid, respectively; $\gamma_S^{-}$ and $\gamma_L^{-}$ are the Lewis base components of the asphalt binder and the liquid, respectively.

The cohesive and adhesive energies of the asphalt-aggregate interface were calculated using Eqs. (2) and (3) [42]. For adhesive bond energy, SFE of limestone aggregate was selected from the previous study and evaluated using Eq. (3) [44]. The SFE components of the test liquids and limestone for asphalt are detailed in Table 2.

$$\Delta G_{11} = \Delta G_{11}^{LW} + \Delta G_{11}^{AB} = 2\gamma_1^{LW} + 4\sqrt{\gamma_1^{+}\gamma_1^{-}} \quad (2)$$

$$\Delta G_{12} = \Delta G_{12}^{LW} + \Delta G_{12}^{AB} = 2\sqrt{\gamma_1^{LW}\gamma_2^{LW}} + 2\sqrt{\gamma_1^{+}\gamma_2^{-}} + 2\sqrt{\gamma_1^{-}\gamma_2^{+}} \quad (3)$$

Where the subscripts 1 and 2 refer to the asphalt and aggregates, respectively.

### 3.4. Rotational viscometer (RV)

The rotational viscosity (RV) test, performed using a Brookfield viscometer, measures the flow characteristics of the asphalt binders at elevated temperatures to assess its workability. This test determines suitable temperatures for asphalt construction and enables the evaluation of activation energy characteristics. RV testing was conducted at 120 °C, 135 °C, 150 °C, and 177 °C using a 27# rotor according to ASTM D4402–06 standard [45]. As asphalt binders are heated, they undergo viscous flow, a process driven by thermal activation. To characterize the binder's resistance to flow and workability, flow activation energy ($E_v$) was employed. The relationship between viscosity and temperature was evaluated using the Arrhenius equation to determine $E_v$.

### 3.5. Rheological testing

The rheological properties of various asphalt binders were analyzed using a TA Instruments Discovery Hybrid Rheometer (DHR). This assessment involved multiple stress creep and recovery (MSCR) tests along with time sweep tests.

MSCR tests were performed on asphalt samples at 64 °C, applying stress levels of 0.1 kPa and 3.2 kPa. The tests measured percent recovery ($R\%$) and non-recoverable creep compliance ($J_{nr}$) in accordance with AASHTO TP 70 [46].

Time sweep tests were performed to evaluate fatigue properties using a parallel plate with a 2 mm gap and an 8 mm diameter. Non-destructive tests at 0.1 % strain and destructive tests at 5 % strain were conducted at a fixed frequency of 10 Hz across temperatures of 15 °C, 20 °C, and 25 °C. Shear modulus and phase angle were monitored to analyze the dynamic behavior and fatigue characteristics of asphalt binders.

### 3.6. Pull-off strength test

A Dynamic Testing System (DTS) machine was utilized to carry out the pull-off test, aimed at evaluating the adhesion performance of asphalt. The test was performed at 20 °C with a loading rate of 0.7 MPa/s. Small cylindrical limestone samples were used for their uniformity. The testing setup included a bottom holder for the limestone and a top steel stub designed to apply a precise asphalt film, as done in previous studies [47]. Limestone samples and steel stubs were cleaned with distilled water and reheated to 200 °C before applying pre-weighed asphalt, which was spread evenly and cured for 30 min at 20 °C [47,48]. The asphalt mass was calculated using the formula:

$$m = \pi r^2 t\rho \quad (4)$$

Where $m$ is the mass of asphalt; $r$ is the radius of the circular area on the limestone; $t$ is the asphalt film thickness; $\rho$ is the asphalt density.

**Table. 1**
Rejuvenated binders with different additive contents.

| No | Different contents of additive for rejuvenation |
|---|---|
| M1 | PB + 7.5 % WEO + 6 % CR + 2 % SBS |
| M2 | PB + 7.5 % WEO + 6 % CR + 3 % SBS |
| M3 | PB + 10 % WEO + 6 % CR + 2 % SBS |
| M4 | PB + 10 % WEO + 6 % CR + 3 % SBS |

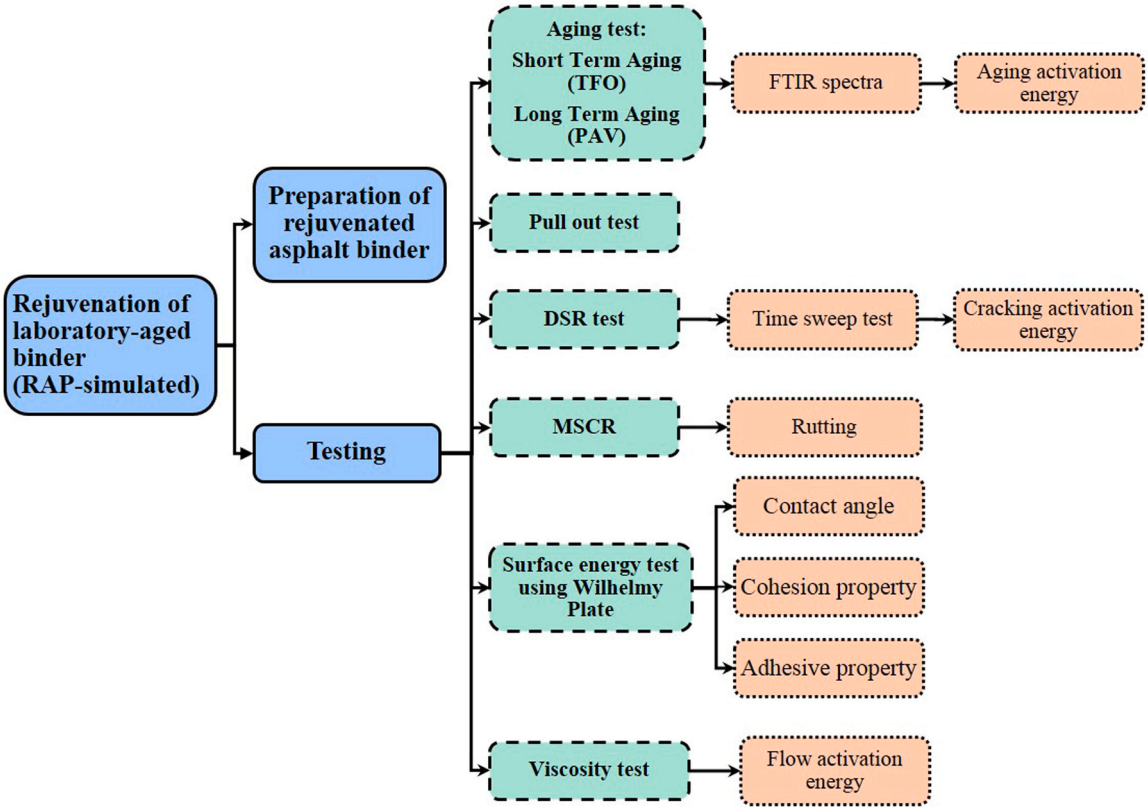


**Fig. 2.** Flow Chart for Experimental plan and Evaluation Method.

**Table. 2**
SFE components of test liquids and limestone for asphalt ($mJ/m^2$).

| Liquid | $\gamma_S$ | $\gamma^{LW}$ | $\gamma^{AB}$ | $\gamma^+$ | $\gamma^-$ |
|---|---|---|---|---|---|
| Distilled water | 72.8 | 21.8 | 51 | 25.5 | 25.5 |
| Glycerol | 64.0 | 34.0 | 30 | 3.92 | 57.40 |
| Formamide | 58.0 | 39.0 | 19 | 2.28 | 39.60 |
| Limestone | 49.8598 | 49.3293 | 0.527 | 0.0054 | 12.8407 |

Fig. 3 illustrates the test samples and experimental setup used in this study.

## 4. Results and discussions

### 4.1. Calculation of carbonyl content

The PB and rejuvenated binders are indicated by the intensities of carbonyl (1650–1800 $cm^{-1}$) and sulfoxide (950–1050 $cm^{-1}$) peak areas,

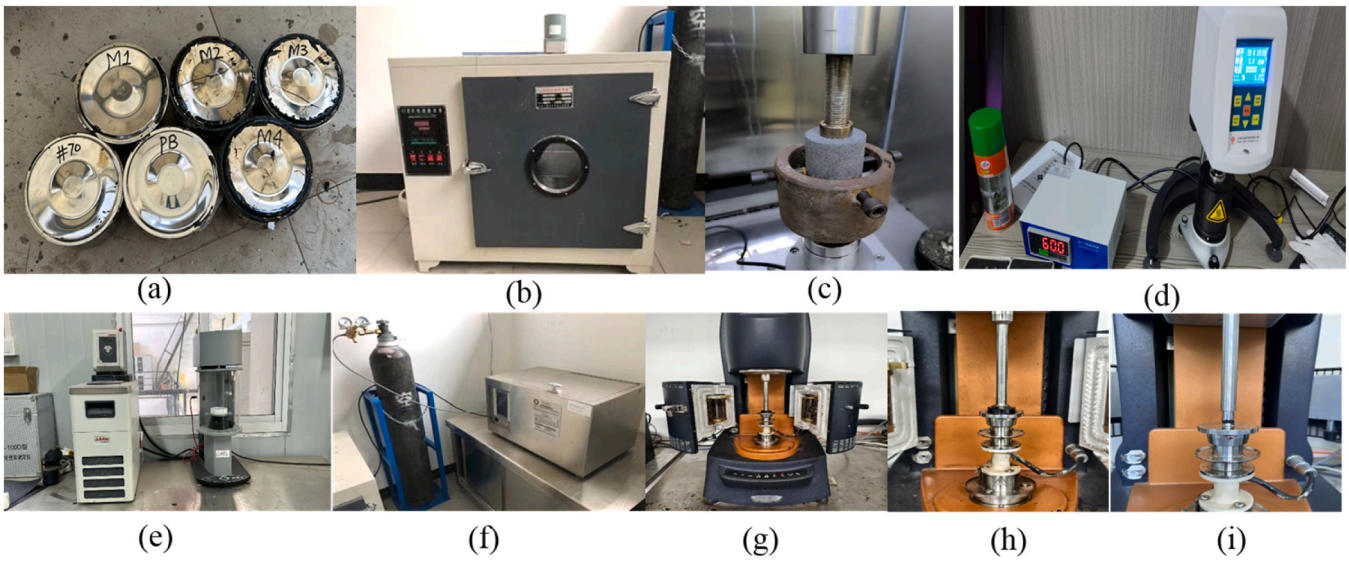


**Fig. 3.** Test samples and experimental setup: (a) asphalt binder samples, (b) Thin Film Oven (TFO), (c) pull-off strength test, (d) rotational viscometer (RV), (e) surface energy test using Wilhelmy plate method, (f) Pressure Aging Vessel (PAV), (g) dynamic shear rheometer (DSR), (h) DSR MSCR test sample, (i) DSR fatigue test sample.

where elevated levels indicate asphaltene accumulation and binder aging. PB exhibited the highest indices of these functional groups due to oxidation and volatilization, while the 70# binder have lower carbonyl content. The introduction of rejuvenators into the blend substantially reduces the carbonyl and sulfoxide indices of the binders [49], demonstrating their effectiveness in mitigating aging effects and stabilizing functional groups, as shown in Fig. 4. Notably, formulations with higher rejuvenator content, such as M4, show a more significant decrease in these indices, indicating enhanced binder softening due to increased maltene content and a reduced asphaltene fraction. This reduction suggests improved resistance to aging and a decrease in carbonyl content, with no change in absorption peak positions, implying that rejuvenation primarily involves physical interactions rather than chemical modifications [11,50].

The degradation of CR and the absorption of WEO light fractions by CR and SBS improve elasticity, compatibility, and promote an increase in soluble fractions, thereby reducing crosslinking density and enhancing compatibility with the PB binders [51]. FTIR analysis revealed that the incorporation of rejuvenators influences peak intensities, particularly by reducing the carbonyl (C═O) and sulfoxide (S═O) functional group content, indicating mitigation of oxidative aging effects (Fig. 4). The incorporation of WEO restores the colloidal structure by increasing maltene content and adjusting the asphaltene-to-maltene ratio, which improves workability and reduces carbonyl content. Simultaneously, swelling of CR particles and their interaction with SBS form a stable gel-phase structure, enhancing the cohesive energy of the binder and improving its fatigue resistance [19,51].

However, excessive maltene restoration at high WEO content (10 %) disrupts the colloidal stability of the binder, causing over-softening and a notable reduction in carbonyl content. This imbalance likely diminishes the synergistic benefits of combining rejuvenators. The dominance of light components (maltenes) lowers the binder's stiffness, increases susceptibility to rutting and deformation [23,52].

### 4.2. Calculation of kinetic oxidative aging and activation energy

Aging, accelerated by prolonged environmental exposure and high temperatures, is characterized by rapid and constant carbonyl growth rates, which are critical for determining aging kinetics [53]. The dual phases of oxidative aging, characterized by rapid and constant-rate periods, are described using the Arrhenius equations (Eqs. (5)-(7) [29,54].

$$CA = CA_i + (CA_0 - CA_i)(1 - e^{-k_f t}) + k_c t \quad (5)$$

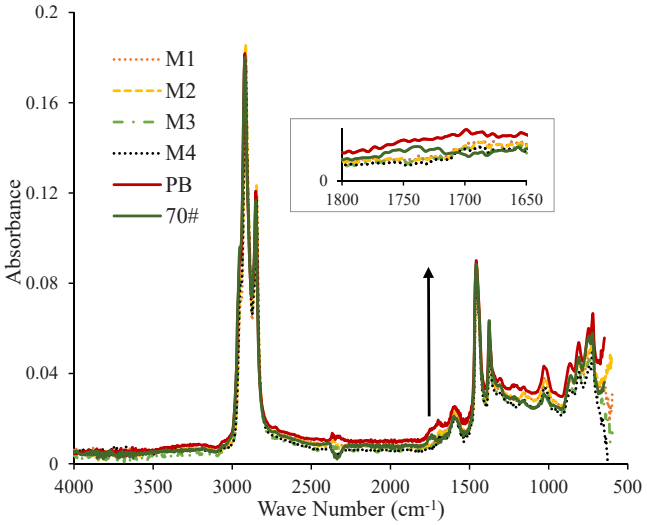


**Fig. 4.** Infrared spectra of asphalt binders.

$$k_f = A_f e^{-E_{af}/RT} \quad (6)$$

$$k_c = A_c e^{-E_{ac}/RT} \quad (7)$$

Where $CA$ is the carbonyl content; $CA_i$ is the initial carbonyl content; $CA_0$ is the intercept of the constant-rate line; $t$ is the oxidative aging time; $A_f$ is the pre-exponential factor, $E_{af}$ is the activation energy, and $k_f$ is the reaction rate constant for the fast reaction period; $A_c$ is the pre-exponential factor; $E_{ac}$ is the activation energy; and $k_c$ is the reaction rate constant for the constant reaction period.

Kinetics-based modeling advances our understanding of asphalt binder reaction mechanisms. The increase in CA within the spectral range of 1650 $cm^{-1}$ and 1820 $cm^{-1}$ , calculated at different temperatures using Eq. (5), were used to assess the kinetic parameters of oxidative aging in rejuvenated binders. For long-term analysis, the constant CA reaction rate is especially significant, as it reflects the material's behavior during advanced service life.

$$\Delta CA = \Delta CA_{\infty}^{-(\rho_c/t)^{\beta_c}} \quad (8)$$

Where $\Delta CA_{\infty}$, $\rho_c$ and $\beta_c$ are fitting parameters calculated for binders using the optimization method utilizing Excel Solver. The representative rate of change of $\Delta CA$ for long-term aging is explained as follows:

$$k_{\Delta CA} = \Delta CA_{\infty} \cdot \beta_c \quad (9)$$

The Arrhenius equation is:

$$\ln(k_{\Delta CA}) = \ln(A_{\Delta CA}) - \frac{E_{aa}}{RT} \quad (10)$$

Where $E_{aa}$ is the aging activation energy; $A_{\Delta CA}$ is the pre-exponential factor related to the Constant reaction rate period; $R$ is the gas constant (8.314 J/mol·K); and $T$ is the temperature in Kelvin.

As aging temperature increases, the reaction rate constant ($k_c$) increases, demonstrating high sensitivity to temperature variations. Higher activation energy values imply lower temperature sensitivity, indicating that minor temperature fluctuations exert less influence on reaction rates. Among the rejuvenated binders, M3 and M4 exhibited higher overall carbonyl accumulation during aging, which can be attributed to their greater WEO content (10 %). Their initial carbonyl area values, however, were lower than those of M1 and M2, likely due to the presence of lighter WEO fractions, which volatilize during aging and accelerate subsequent oxidation. In contrast, M2 showed a more gradual and less steep increase in carbonyl content across both time and temperature as compared to other binders, indicating a slower oxidation rate and improved stability. This behavior is likely due to the synergistic effect of its SBS content and balanced WEO dosage, which together promote a stable polymer network that resists oxidative aging. Overall, the increase in WEO content, as seen in Fig. 5, reduces the carbonyl content, lowers the kinetic barrier for the reaction rate, and correlates with a decrease in $E_{aa}$. In Fig. 5, "Meas" denotes the experimentally measured carbonyl area (CA), while "Pred" represents the values predicted by the CA model.

M2 exhibits a higher $E_{aa}$ compared to M1 (Fig. 6). The increased SBS content raises $E_{aa}$, reducing temperature sensitivity [55]. This variation underscores the intricate interplay between additives in modulating the temperature sensitivity of the aging process. Notably, PB exhibits the highest $E_{aa}$ (95.36 kJ/mol), attributed to the elevated concentration of polar molecules and a deficiency of active molecules to react with oxygen. These strong intermolecular forces require more energy to overcome, resulting in higher activation energy [56].

However, the $E_{aa}$ of M2 (84.328 kJ/mol) surpasses that of other rejuvenated binders, following the sequence: PB > M2 > M1 > M4 > M3. This phenomenon is explained by the SBS-CR interactions within the binder. The light components introduced by WEO are absorbed by the polymers, leading to the formation of a stable

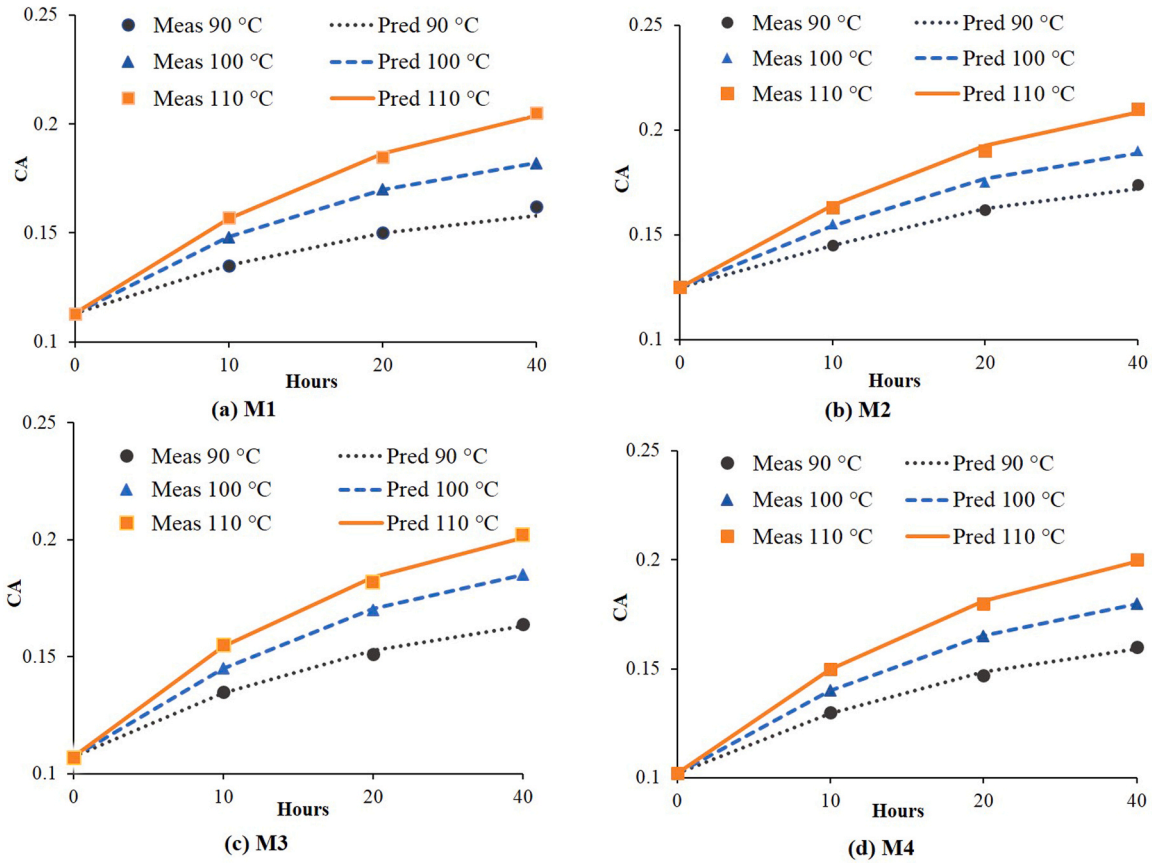


**Fig. 5.** CA of rejuvenated asphalt binder at various temperatures and time periods.

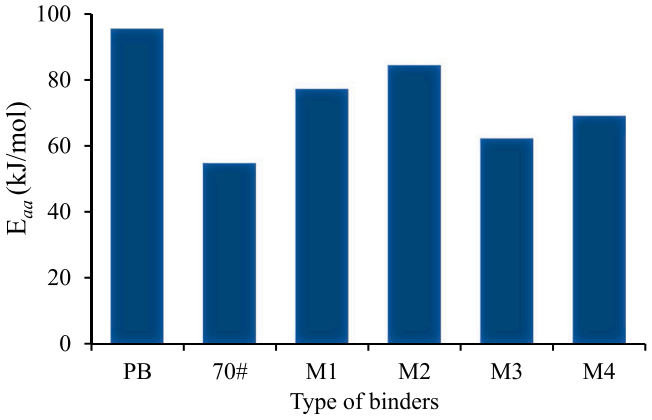


**Fig. 6.** Aging Activation energy ($E_{aa}$) of asphalt binders.

network and larger molecular structures, which enhances the binder's ability to resist oxidation [40]. Specifically, the polymeric network formed by SBS and CR increases the binder's resistance to aging, resulting higher $E_{aa}$ for M2.

On the other hand, when a higher amount of WEO is added, as seen in M3 and M4, the increase in light components accelerate oxidation, causing a decrease in $E_{aa}$. In contrast, M1 and M2, which have lower WEO content, exhibit higher oxidation resistance due to the lower presence of light components and a higher concentration of polymeric structures compared to M3 and M4. The low light components and high polymeric structure formed by polymers contribute to a higher $E_{aa}$ of M2 and M4.

### 4.3. Calculation of pseudo strain energy-based kinetic cracking model

Fatigue damage in asphalt binders is evaluated using the cumulative dissipated pseudo strain energy (DPSE), which is crucial because it quantifies the cumulative energy dissipation of asphalt under shear loading while excluding the viscous effects, as per Schapery's elastic-viscoelastic correspondence principle [57]. The apparent pseudo-shear strain $\gamma_R^A(t,r)$ is determined by:

$$\gamma_R^A(t,r) = \frac{\int_0^t G^A(t-\xi)\frac{d\gamma^A(\xi,r)}{d\xi}d\xi}{\left|G_R^{*A}\right|} \tag{11}$$

Where $\gamma_R^A(t,r)$ is the apparent shear pseudo strain; $G^A(t-\xi)$ is the relaxation modulus; $\frac{d\gamma^A(\xi,r)}{d\xi}d\xi$ is the rate of change of the apparent shear strain; $\left|G_R^{*A}\right|$is the reference modulus.

The apparent shear stress and strain in the asphalt binder at any particular point $r$ is explained as follow:

$$\gamma^A(t,r) = \gamma_0^A(t_0,r)sin(\omega t) = \frac{\theta_0^A}{h}rsin(\omega t) \tag{12}$$

$$\tau^A(t,r) = \tau_0^A sin(\omega t + \delta^A) \tag{13}$$

By integrating the apparent pseudo shear strain across the material's volume and applying

the equation for apparent shear stress, the dissipated pseudo strain energy $DPSE_c^A$ $(t)$ is calculated using Eq. (14):

$$DPSE_c^A(t) = \iiint_{V^c}\left[\int_{t_0}^{t_0+2\pi/\omega}\tau^A\left(t,r\right)d\gamma_R^A\left(t,r\right)\right]dV \tag{14}$$

Where $V^c$ is the volume of asphalt failure caused by cracking; $\tau^A(t,r)$ is

the apparent shear stress at any loading time $t$ and radius $r$.

The accumulated dissipated pseudo strain energy caused by cracking $DPSE_c$ , is calculated as follows:

$$D_{DPSE_c} = \sum_{0}^{t_N} DPSE_c^A(t) \tag{15}$$

Where $t_N$ is the final loading time.

The three-parameter model fit the curve with the calculated value of$D_{DPSE_c}$, with parameters optimized via Excel Solver:

$$D_{DPSE_c} = D_{DPSE_\infty} e^{-\left(\frac{\rho_{ca}}{t}\right)^{\beta_{ca}}} \tag{16}$$

Where $D_{DPSE\infty}$ represents the maximum value that $DPSE_c$ of asphalt binder can reach under the action of controlled shear load; $\rho_{ca}$represents a proportionality factor on the horizontal axis; and $\beta_{ca}$characterizes the representative rate of change of $D_{DPSEc}$.

The rate constant $\beta_{ca}$ is expressed using the Arrhenius equation [32]:

$$\beta_{ca} = A_{ca} e^{-E_{ac}/RT} \tag{17}$$

Taking the natural logarithm of both sides of Eq. (17) yields:

$$\ln(\beta_{ca}) = \ln(A_{ca}) - \frac{E_{ac}}{RT} \tag{18}$$

The representative energy change rate $(\beta_{ca})$ during the damage stage is plotted as $\ln(\beta_{ca})$ against 1/RT, where the slope represents the cracking activation energy $E_{ac}$ [29].

As shown in Fig. 7, the PB binder exhibits higher $D_{DPSEc}$ and is more susceptible to cracking at 20 °C compared to other binders. However, the inclusion of WEO, CR, and SBS in PB leads to a notable reduction in cumulative $DPSE_c$, indicating improved fatigue resistance and enhanced durability of the binder under cyclic loading conditions.

The calculated and predicted values of accumulated $DPSE_c$, obtained under dynamic loading conditions and leading to fatigue cracking in different asphalt samples, are illustrated in Fig. 8**.** The dashed lines represent the predicted $DPSE_c$ derived from the three-parameter $D_{DPSE\ \ c}$model. The fitting curves exhibit a close alignment with experimentally measured $DPSE_c$ across various binder types, affirming the model's accuracy and reliability. $DPSE_c$ increases with loading time, though the rate of increase diminishes progressively. Increasing the content of WEO and SBS in the rejuvenated binders resulted in a continued decrease in accumulated $DPSE_c$. While $DPSE_c$ generally increases with loading time, it decreases at relatively higher temperatures within the tested range (i.e., 20 °C–25°C), corresponding to reduced fatigue cracking rate.

By applying $DPSE_c$ to quantify fatigue damage in asphalt binders, a kinetic analysis examines the correlation between temperature and the rate of $DPSE$ change $(\beta_{ca})$. The representative change rate $(\beta_{ca})$ of

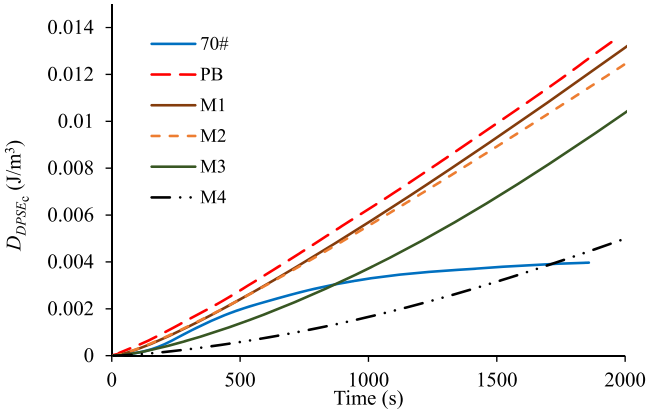


**Fig. 7.** *DSPE* cracking of different asphalt samples at 20 °C.

accumulated $DPSE_c$ during the damage phase is analyzed using an Arrhenius plot of $\ln(\beta_{ca})$ verses 1/RT, enabling to calculate the cracking activation energy $(E_{ac})$ [29,32].

Fig. 9 reveals that the PB binder has the lowest $E_{ac}$, which is associated with a shorter fatigue life and a higher level of fatigue damage. This is likely due to increased agglomeration of asphaltene content and polar molecules, which causes stronger interaction and enhances binder stiffness [58]. In contrast, the M4 binder, with higher SBS and WEO rejuvenator content, exhibits the highest $E_{ac}$ (85.34 kJ/mol), indicating improved resistance to cracking. The sequence of $E_{ac}$ values is as follows: M4 > M3 > 70# > M2 > M1 > PB. This increase in $E_{ac}$ in M4 is due to the recovery of maltene content and the formation of a stable network structure, enhancing the $E_{ac}$ of the PB binder from 30.73 kJ/mol to 85.34 kJ/mol. This indicates that higher rejuvenator content enhances the cracking resistance of PB binders [8,58].

### 4.4. MSCR test result

The MSCR test was employed to characterize asphalt at 64 °C under stress levels of 0.1 kPa and 3.2 kPa, evaluating two critical rutting parameters: non-recoverable creep compliance $(J_{nr})$ and percentage of recovery $(R\%)$ [59,60]. These parameters are calculated as follows:

$$R\% = \frac{\varepsilon_1 - \varepsilon_{10}}{\varepsilon_1} \tag{19}$$

$$J_{nr} = \frac{\varepsilon_{10}}{\sigma} \tag{20}$$

Where$\sigma$ is the applied shear stress;$\varepsilon_{10} = \varepsilon_r - \varepsilon_0$represents the net residual strain;

$\varepsilon_1 = \varepsilon_c - \varepsilon_0$represents the net creep strain;$\varepsilon_0$represents initial creep strain for each cycle; $\varepsilon_r$represents the final strain in the recovery stage for each cycle; $\varepsilon_c$represents the strain at the end of the creep phase.

The stress level significantly influenced the $R\%$ and $J_{nr}$ values of asphalt samples. Under 0.1 kPa stress, samples M3 and M4 showed higher strain values compared to M1 and M2, as shown in Fig. 10(a). In contrast, under a 3.2 kPa stress, all binders showed increased $J_{nr}$ and decreased $R\%$ values, as illustrated in Fig. 10(b). The PB binder, in particular, exhibited the highest $R\%$ and the lowest $J_{nr}$, with minimal influence from the increased stress, indicating superior deformation resistance and elastic performance due to enhanced stiffness [61].

Binder M2 demonstrated higher $R\%$ and lower $J_{nr}$ at 0.1 kPa, indicating superior rutting resistance under light traffic compared to other rejuvenated binders. Similarly, under 3.2 kPa stress, M2 exhibited lower $J_{nr}$, confirming its superior high-temperature performance. In contrast, M4 showed higher $J_{nr}$ at 3.2 kPa and 64 °C, while M2 had the lowest $J_{nr}$ among the rejuvenated binders. The binders are ranked for $R\%$ at both stress levels (0.1 kPa and 3.2 kPa) as follows: PB > M2 > M1 > M4 > M3 > 70#.

Higher WEO content in M3 and M4 increased the maltene fraction, softening the binder and raising $J_{nr}$ values [14]. M3 exhibited lower R% and lower $J_{nr}$ than M4, whereas the excessive WEO in M4 counteracted the benefits of SBS, resulting in higher $J_{nr}$ and R% compared to M3. The higher SBS content in M2 and M4 enhanced $R\%$ compared to M1 and M3. Among all rejuvenated binders, M2 showed the lowest $J_{nr}$ and the highest $R\%$, confirming its superior rutting resistance.

The addition of SBS and CR enhanced elasticity by forming a cross-linked polymer network, partially mitigating the softening effect of WEO [40,62]. Despite this improvement, excessive WEO reduced binder stiffness and deformation resistance, highlighting the importance of dosage balance. Overall, rutting susceptibility decreases with a reduction in $J_{nr}$, while $R\%$ reflects the elastic recovery ability of the binder, where higher values indicate superior elasticity. $J_{nr}$ increased and $R\%$ decreased for all binders as the stress level increased (Fig. 10(b)).

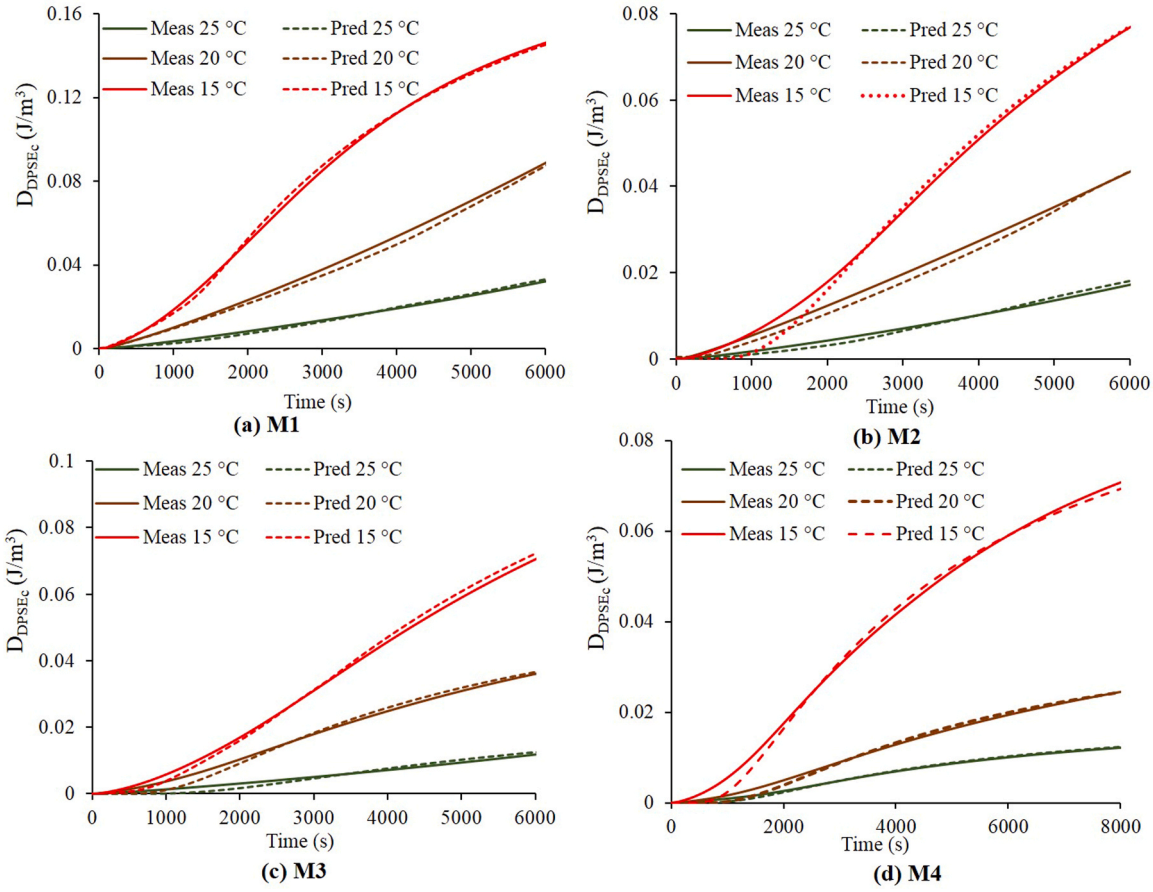


**Fig. 8.** *DPSE* cracking, both measured and predicted, for rejuvenated binders at various temperatures.

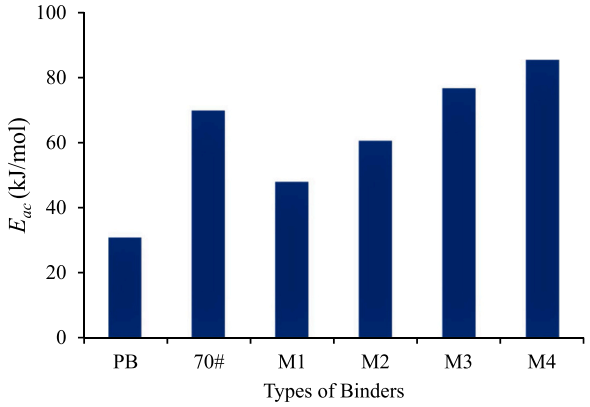


**Fig. 9.** Activation energy for cracking of different binders.

### 4.5. Viscous flow and rotational viscosity test result

The viscous flow behavior of the asphalt binders across a broad temperature spectrum was evaluated using rotational viscosity tests. Viscosity measurements were conducted at 120 °C, 135 °C, 150 °C, and 177 °C (Fig. 11). Viscosity, defined as a fluid's resistance to deformation, is significantly influenced by temperature, aging, and the type of additives used. Among the binders, PB exhibited the highest viscosity, while 70# showed the lowest. This difference is attributed to the higher polar components content in PB, which increased intermolecular forces and viscosity [63].

The addition of WEO and CR to the PB binder resulted in a notable reduction in viscosity. Conversely, increased SBS content elevated viscosity, highlighting the role of additive type in governing the binder's resistance to flow [64]. Increasing the content of rejuvenators (WEO, CR, and SBS) significantly influenced variations in stiffness, particularly at higher concentrations, compared to binders using equivalent amounts of WEO and CR. Moreover, increasing the WEO content reduces viscosity, which is advantageous during the mixing process.

At low temperatures, the addition of WEO significantly reduces viscosity. However, this effect diminishes at elevated temperatures (177 °C), where the viscosity differences between binders became less pronounced. The decrease in viscosity at elevated temperatures is attributed to the reduction of intermolecular forces, illustrating the inverse relationship between temperature and viscosity due to increased molecular motion. These findings highlight the significant impact of temperature on the flow properties of asphalt binders, with additives inducing measurable changes in viscosity.

#### 4.5.1. Viscous flow activation energy ($E_v$)

The temperature sensitivity of asphalt binder viscosity is clarified by the viscous flow activation energy ($E_v$), which is pivotal in understanding the binder's resistance to flow. Using rheological kinetics, the relationship between viscosity and temperature is assessed across various temperature ranges and described by the Arrhenius equation:

$$\eta = Ae^{\frac{E_v}{RT}} \tag{21}$$

Applying logarithm on both sides of Eq. (21), we obtain:

$$\ln\eta = \frac{E_v}{RT} + \ln A \tag{22}$$

Where $\eta$ is the viscosity; $A$ is the pre-exponential factor; $E_v$ is the activation energy of viscous flow in kJ/mol; $T$ is the absolute temperature in

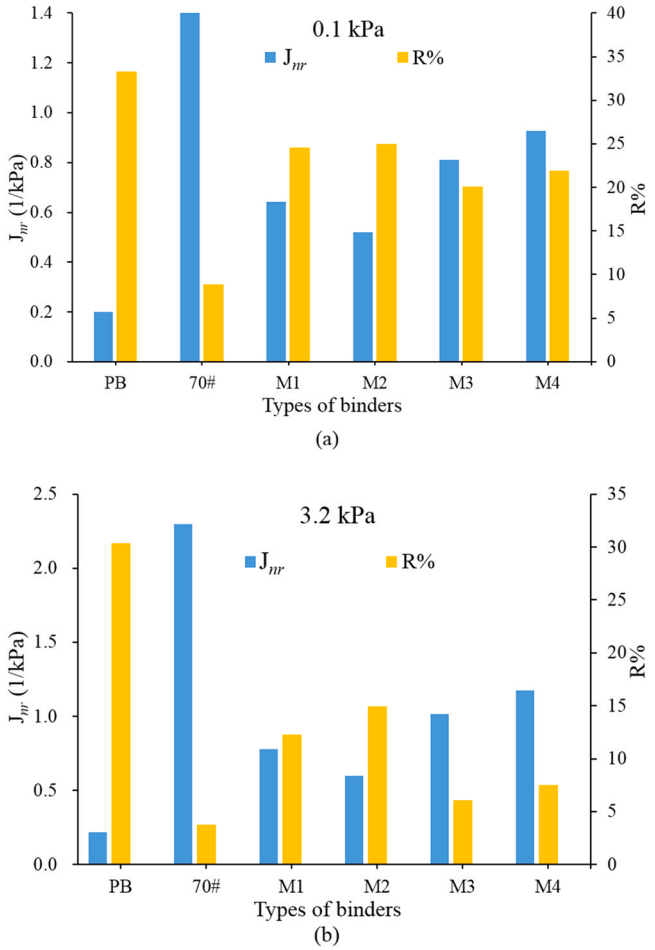


**Fig. 10.** $J_{nr}$ and R% Results for asphalt samples MSCR test, (a) 0.1 kPa, (b) 3.2 kPa.

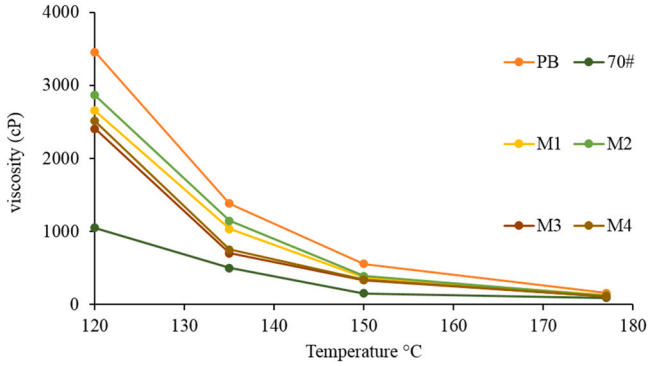


**Fig. 11.** Viscosity Test of asphalt binders at various temperatures.

K; $R$ is the gas constant, 8.314 J/(mol·K).

As temperature increases, the intermolecular forces in binder weaken, reducing the energy required to initiate viscous flow. This leads to a decrease in viscosity, which aligns with the well-established inverse relationship between temperature and viscosity as described by the Arrhenius model. The PB binder exhibits the highest $E_v$ (82.1 kJ/mol, Table 3) indicating greater temperature stability compared to rejuvenated binders. This can be attributed to the increased concentration of polar molecules due to aging, enhanced polarity, and promoted stronger intermolecular adhesion bonds within the binder matrix, thereby stabilizing its structure, resulting in higher viscosity and activation energy compared to other binders [63,65].

**Table. 3**
Flow activation energy of different binders.

| Type of binders | Arrhenius Model (ln$\eta$–1/T) | $E_v$ (kJ/mol) |
|---|---|---|
| PB | y = 9874.2x - 16.945 | 82.1 |
| 70# | y = 7289.8x - 10.959 | 60.6 |
| M1 | y = 9417.1x - 16.155 | 78.3 |
| M2 | y = 9585.5x - 16.425 | 79.69 |
| M3 | y = 9106.2x - 15.63 | 75.97 |
| M4 | y = 9322.3x - 16.026 | 77.5 |

The reduction of intermolecular forces at elevated temperatures directly accounts for the viscosity reduction in asphalt binders. $E_v$, calculated from the Arrhenius relationship between viscosity and temperature, serves as a quantitative measure of the binder's resistance to flow under thermal stress. When compared to the base 70# binder, the incorporation of SBS and CR, particularly at higher SBS content, resulted in increased $E_v$ value, as seen in M2 (79.7 kJ/mol) and M4 (77.5 kJ/mol), signifying enhanced viscosity.

The incorporation of WEO reduces both viscosity and $E_v$. Thus, $E_v$ serves as a comprehensive indicator of temperature-dependent rheological properties, offering critical insights into how the binder's chemical structure and aging influence its performance.

### 4.6. *Bonding properties of asphalt*

The asphalt binder's surface free energy (SFE), including dispersion and polar components, was evaluated using Eq. (1). Aging significantly reduces the SFE, leading to a net reduction in the dispersion component. For instance, the PB binder exhibited lower SFE (13.77 mJ/m$^2$) compared to 70# binder (16.89 mJ/m$^2$), attributed primarily to an amplified ratio of asphaltenes and the polar component [66], alongside a decrease in Lifshitz-van der Waals component, as shown in Fig. 12.

However, incorporating WEO, SBS, and CR into the PB binder restores its SFE. These additives revitalize the aged asphalt's colloidal structure and enhance the SFE components by increasing the proportions of both Lifshitz-van der Waals and polar components. WEO contributes by increasing the lighter components and restoring the colloidal structure, while its absorption by elastic polymers forms a gel-phase structure, further improving the binders adhesion performance [67]. Increasing the WEO content enhances the polar component, whereas the addition of SBS and CR primarily increases the Lifshitz-van der Waals component, leading to an overall increase in total surface energy. Through the incorporation of these additives, the SFE of the binders (M1 to M4) increased from 18.513 mJ/m$^2$ to 21.304 mJ/m$^2$, as shown in Fig. 12. M4 exhibited the highest SFE (21.304 mJ/m$^2$) due to the higher additive dosage, while M1 had the lowest SFE (18.513 mJ/m$^2$).

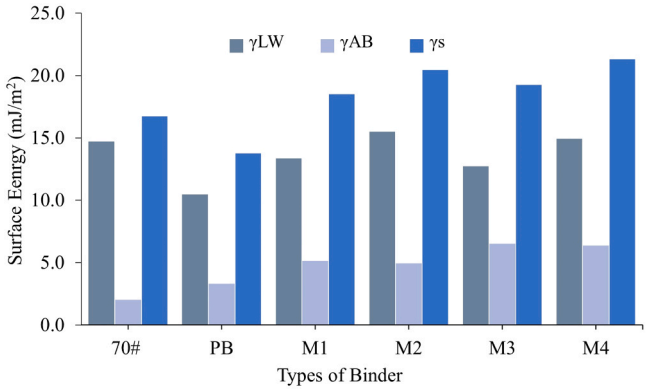


**Fig. 12.** Surface energy and its components of different binders.

Cohesion energy, an intrinsic property of the binder, signifies the energy necessary to split two binder layers into distinct surfaces. Adhesion energy, which reflects the compatibility between the binder and aggregate surfaces, is required to separate them and is calculated using Eqs. (2) and (3).

As WEO and SBS are incrementally added, viscosity changes along with changes in the dispersion and polar components. The dispersive component becomes the predominant factor in the asphalt SFE. Higher dispersive components indicate stronger adhesion, leading to increased SFE, cohesive energy, and adhesive energy [20,64], as depicted in Fig. 13.

Cohesive energy exhibits a similar trend to SFE, following the sequence: M4 > M2 > M3 > M1 > 70# > PB, as shown in Fig. 13. Additives amplify cohesion with an increase in concentration, thereby improving the work of cohesion of PB from 27.55 mJ/m$^2$ to 42.61 mJ/m$^2$. Among the rejuvenated binders, M4 (42.61 mJ/m$^2$) exhibited the highest cohesion due to the higher additive content.

Limestone aggregate, known for its high adhesive properties and basic nature compared to other aggregates, significantly contributes to the adhesion work with the rejuvenated binders [68]. The characteristics of limestone, together with the increase in additive content in the binders, enhance the SFE polar components, particularly acid-base interactions. The light components provided by WEO in the asphalt binder are absorbed by CR and SBS, forming an interconnected network structure that enhances the adhesion performance [69]. This results in stronger adhesive bonds between the rejuvenated binder and alkaline limestone aggregate due to improved wettability and enhanced molecular interactions at the interface, leading to an increase in adhesion-free energy [21]. This follows a similar trend to cohesive energy and surface energy, as illustrated in Fig. 13**.** It suggests that increasing the additive content in PB enhances the light components and SFE, ultimately improving the bonding properties of the binders.

### 4.7. *Pull-off Strength*

Fig. 14 illustrates the pull-off strength (POTS) of asphalt samples with limestone aggregates. The POTS of the PB binder is lower than that of the 70# binder due to increased stiffness, which aligns with the surface energy results. An increase in POTS values for limestone aggregate was observed with the addition of rejuvenators to the PB. The tensile strength of the rejuvenated binders shows a notable increase compared to that of the PB binder, with a 53.05 % increase for M1 and a 39.71 % increase for M4. This improvement is attributed to increased molecular diffusion and superior inner cohesion in the rejuvenated binders compared to PB binders.

The addition of WEO, in combination with CR restores the PB colloidal structure, augments CR swelling and increases resin content. The addition of SBS forms a gel phase and creates a cross-linked stable mesh, thereby improving adhesion performance and increasing POTS [21,69].

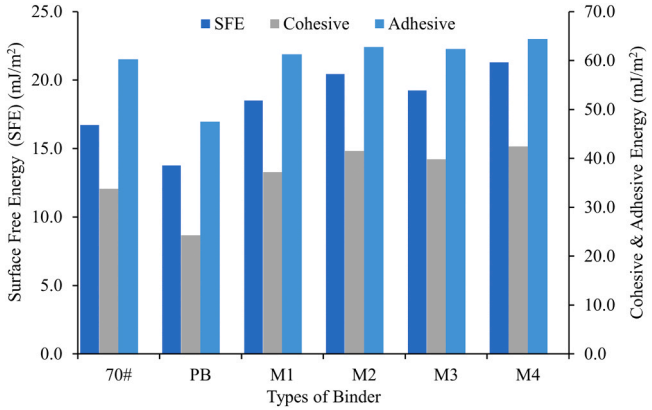


**Fig. 13.** Surface, Adhesive, and Cohesive Energies of different Asphalt binders.

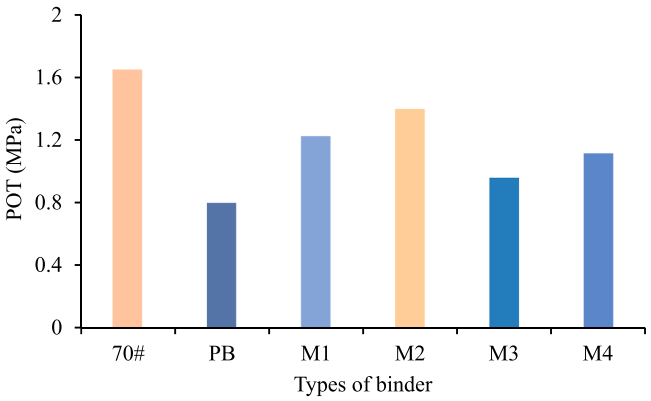


**Fig. 14.** Pull-off strength of different asphalt types and limestone aggregate.

The reduction in PB binder stiffness due to WEO addition enhances POTS by reducing asphalt brittleness and improving adhesion [70]. However, increasing the WEO content introduces more light components, which soften the binder, leading to a decrease in POTS and performance, as shown in Fig. 14 [71].

Nevertheless, all rejuvenated binders exhibited higher bond strength than the PB binder. The findings suggest that adding 7.5 % WEO increases the light components, which is absorbed by CR and SBS to form a colloid structure with the PB binder. Overall, the incorporation of WEO, CR, and SBS in PB binders significantly enhances bond strength.

## 5. Conclusion

This research investigates the aging, cracking, rheological, and bonding characteristics of laboratory-aged binders (PB) used to simulate RAP binders, rejuvenated with different additive contents. A 70-penetration grade asphalt binder (70#) was artificially aged in the laboratory to simulate long-term oxidative aging, producing the PB binder. Four rejuvenated binders were prepared by incorporating different additive systems (6 % CR, 7.5 % and 10 % WEO, and 2 % and 3 % SBS) into PB, and their performance was compared to 70# and PB binders. A series of tests, including FTIR measurements, rheological analysis, contact angle, and pull-off tests, were conducted to analyze the chemical, rheological, and adhesive bond properties of the binders. FTIR was used to analyze asphalt samples after PAV aging at various temperatures and durations to assess resistance to oxidative aging. Time sweep tests were conducted at 15 °C, 20 °C, and 25 °C to evaluate the mechanical performance of binders. The analysis established correlations between FTIR results, aging behavior, rheological characteristics, and adhesion properties. Furthermore, pull-off tests and contact angle measurements were used to investigate cohesive and adhesive failures at asphalt-aggregate interfaces. The results offer valuable insights into the longevity and effectiveness of rejuvenated asphalt binders, promoting more sustainable pavement materials.

The key findings of this study are as follows:

1) Higher WEO content increases active molecules and temperature sensitivity, reducing the kinetic barrier to oxidation and aging activation energy. However, the incorporation of CR and SBS, due to their polymeric network structure, mitigates temperature sensitivity, indicating an increased kinetic barrier to oxidation and a corresponding rise in aging activation energy ($E_{aa}$).
2) The incorporation of additives influenced the cracking behavior of the rejuvenated binders. The highest fatigue resistance was noted in M4 (10 % WEO, 6 % CR, and 3 % SBS), where higher WEO and SBS content led to elevated cracking activation energy ($E_{ac}$) and

increased fatigue resistance. Conversely, the PB binder exhibited the lowest $E_{ac}$, indicating higher levels of fatigue damage.

3) Surface energy results suggest that the increased polymer network structure formed by SBS and CR in M2 (7.5 % WEO, 6 % CR, and 3 % SBS) and in M4 (10 % WEO, 6 % CR, and 3 % SBS) asphalt-aggregate systems results in greater adhesive bond properties compared to the higher WEO content in M1 (7.5 % WEO, 6 % CR, and 2 % SBS) and M3 (7.5 % WEO, 6 % CR, and 2 % SBS).
4) According to rheological test results, M2 exhibited improved elastic properties and rutting resistance compared to the other rejuvenated binders. However, the rheological properties degraded markedly with increasing WEO content. In MSCR tests, higher WEO content leads to higher $J_{nr}$ values and lower $R\%$ at elevated temperatures, while the CR-SBS network improves high-temperature performance.
5) The $E_{aa}$ correlates positively with the viscous flow activation energy ($E_v$), underscoring a consistent relationship between the rejuvenator's effect on aging and viscosity characteristics. Additionally, a positive correlation between $E_{ac}$ and surface energy was observed.
6) This study primarily examined the aging, cracking, rheological, and adhesion characteristics of PB binders rejuvenated with WEO, CR, and SBS systems. Future research is recommended to assess the properties of these additives in RAP mixtures to better understand their practical applications.

## CRediT authorship contribution statement

**Jiawei Wang:** Writing – review & editing, Investigation, Formal analysis. **Xue Luo:** Writing – review & editing, Supervision, Resources, Methodology, Funding acquisition, Formal analysis, Conceptualization. **Abdul Samad:** Writing – review & editing, Writing – original draft, Validation, Methodology, Formal analysis. **Muhammad Waheed Abid:** Formal analysis, Review & editing.

## Declaration of Competing Interest

The authors declare that they have no known competing financial interests or personal relationships that could have appeared to influence the work reported in this paper.

## Acknowledgment

The authors gratefully acknowledge the support of the Royal Society under the International Exchanges Scheme, project code IEC\NSFC \223060, and the support of the European Union HORIZON TMA MSCA Staff Exchanges (HORIZON-MSCA-2021-SE-01), grant agreement no 101086071.

## Data availability

Data will be made available on request.

## References

[1] Q. Qin, J.F. Schabron, R.B. Boysen, M.J. Farrar, Field aging effect on chemistry and rheology of asphalt binders and rheological predictions for field aging, Fuel 121 (2014) 86–94, https://doi.org/10.1016/j.fuel.2013.12.040.
[2] F. Xiao, L. Xu, Z. Zhao, X. Hou, Recent applications and developments of reclaimed asphalt pavement in China, 2010–2021, Sustain. Mater. Technol. 37 (2023) e00697, https://doi.org/10.1016/j.susmat.2023.e00697.
[3] G.O. Bamigboye, D.E. Bassey, D.O. Olukanni, B.U. Ngene, D. Adegoke, A. O. Odetoyan, M.A. Kareem, D.O. Enabulele, A.T. Nworgu, Waste materials in highway applications: an overview on generation and utilization implications on sustainability, J. Clean. Prod. 283 (2021) 124581.
[4] G. Xu, H. Wang, Molecular dynamics study of oxidative aging effect on asphalt binder properties, Fuel 188 (2017) 1–10, https://doi.org/10.1016/j.fuel.2016.10.021.
[5] J. Liu, Q. Liu, S. Wang, X. Zhang, C. Xiao, B. Yu, Molecular dynamics evaluation of activation mechanism of rejuvenator in reclaimed asphalt pavement (RAP) binder, Constr. Build. Mater. 298 (2021) 123898.
[6] M. Guo, X. Yin, X. Du, Y. Tan, Effect of aging, testing temperature and relative humidity on adhesion between asphalt binder and mineral aggregate, Constr. Build. Mater. 363 (2023) 129775.
[7] T. Zhou, L. Cao, E.H. Fini, L. Li, Z. Liu, Z. Dong, Behaviors of asphalt under certain aging levels and effects of rejuvenation, Constr. Build. Mater. 249 (2020) 118748, https://doi.org/10.1016/j.conbuildmat.2020.118748.
[8] I. Mohi Ud Din, F.S. Bhat, M.S. Mir, A study investigating the impact of waste cooking oil and waste engine oil on the performance properties of RAP binders, Road. Mater. Pavement Des. 24 (2023) 295–309.
[9] X. Jia, B. Huang, J.A. Moore, S. Zhao, Influence of waste engine oil on asphalt mixtures containing reclaimed asphalt pavement, J. Mater. Civ. Eng. 27 (2015) 4015042, https://doi.org/10.1061/(ASCE)MT.1943-5533.0001292.
[10] Q. Liu, S. Chen, X. He, Y. Su, J. Zeng, Y. Zhu, Y. Pan, B. Zhang, H. Xu, Y. Wu, Surface modification of Fly ash by waste engine oil under mechanical activation enhanced the sustainable service life of asphalt, J. Clean. Prod. 404 (2023) 136785, https://doi.org/10.1016/j.jclepro.2023.136785.
[11] S. Liu, A. Peng, S. Zhou, J. Wu, W. Xuan, W. Liu, Evaluation of the ageing behaviour of waste engine oil-modified asphalt binders, Constr. Build. Mater. 223 (2019) 394–408, https://doi.org/10.1016/j.conbuildmat.2019.07.020.
[12] H.M.R.D. Silva, J.R.M. Oliveira, C.M.G. Jesus, Are totally recycled hot mix asphalts a sustainable alternative for road paving? Resour. Conserv. Recycl 60 (2012) 38–48, https://doi.org/10.1016/j.resconrec.2011.11.013.
[13] G. Mazzoni, E. Bocci, F. Canestrari, Influ. rejuvenators Bitum. Ageing hot Recycl. Asph. mixtures J. Traffic Transp. Eng. (Engl. Ed. 5 (2018) 157–168.
[14] I. Mohi Ud Din, F.S. Bhat, M.S. Mir, A study investigating the impact of waste cooking oil and waste engine oil on the performance properties of RAP binders, Road. Mater. Pavement Des. 24 (2023) 295–309, https://doi.org/10.1080/14680629.2021.2002182.
[15] Z.H. Al-Saffar, H. Yaacob, M.K.I.M. Satar, S.N.N. Kamarudin, M.Z.H. Mahmud, C. R. Ismail, S.A. Hassan, N. Mashros, A review on the usage of waste engine oil with aged asphalt as a rejuvenating agent, Mater. Today Proc. 42 (2021) 2374–2380, https://doi.org/10.1016/j.matpr.2020.12.330.
[16] J.D. Martínez, N. Puy, R. Murillo, T. García, M.V. Navarro, A.M. Mastral, Waste tyre pyrolysis–A review, Renew. Sustain. Energy Rev. 23 (2013) 179–213.
[17] S.A. Tahami, A.F. Mirhosseini, S. Dessouky, H. Mork, A. Kavussi, The use of high content of fine crumb rubber in asphalt mixes using dry process, Constr. Build. Mater. 222 (2019) 643–653, https://doi.org/10.1016/j.conbuildmat.2019.06.180.
[18] X. Yi, R. Dong, M. Zhao, C. Shi, J. Yang, The interaction mechanism and rejuvenation effect of crumb rubber and waste cooking oil blends, Constr. Build. Mater. 302 (2021) 124215, https://doi.org/10.1016/j.conbuildmat.2021.124215.
[19] Y. Zhang, X. Deng, P. Xiao, P. Qian, Y. Zhang, A. Kang, Properties and interaction evolution mechanism of CR modified asphalt, Fuel 371 (2024) 131886.
[20] S. Mohammadi, N. Solatifar, Optimized preparation and high-temperature performance of composite-modified asphalt binder with CR and WEO, J. Mater. Civ. Eng. 35 (2023) 4022395.
[21] X. Kang, R. Wang, J. Yue, X. An, G. Tang, Investigation of the adhesion characteristics of a novel Fast-Melting SBS-Based modifier to Asphalt-Aggregate systems based on a multiscale approach, J. Mater. Civ. Eng. 35 (2023) 4023435.
[22] H. Nan, Y. Sun, J. Chen, M. Gong, Investigation of fatigue performance of asphalt binders containing SBS and CR through TS and LAS tests, Constr. Build. Mater. 361 (2022) 129651.
[23] S.R.M. Fernandes, H.M.R.D. Silva, J.R.M. Oliveira, Developing enhanced modified bitumens with waste engine oil products combined with polymers, Constr. Build. Mater. 160 (2018) 714–724.
[24] J. Xu, J. Pei, J. Cai, T. Liu, Y. Wen, Performance improvement and aging property of oil/SBS modified asphalt, Constr. Build. Mater. 300 (2021) 123735.
[25] L. Xiang, J. Cheng, S. Kang, Thermal oxidative aging mechanism of crumb rubber/SBS composite modified asphalt, Constr. Build. Mater. 75 (2015) 169–175.
[26] S. Ren, X. Liu, W. Fan, C. Qian, G. Nan, S. Erkens, Investigating the effects of waste oil and styrene-butadiene rubber on restoring and improving the viscoelastic, compatibility, and aging properties of aged asphalt, Constr. Build. Mater. 269 (2021) 121338, https://doi.org/10.1016/j.conbuildmat.2020.121338.
[27] Z. Sun, B. Chen, S. Liu, T. Zhou, R. Huang, Polyurethane modified asphalt mixture incorporating waste glass with a wide particle size range: preparation and performance evaluation, Case Stud. Constr. Mater. 20 (2024) e03119.
[28] S. Khan, H. Li, M.H. Ncube, A.A. Butt, Y. Han, J. Harvey, Environmental implications of recycled materials in pavement construction: a comprehensive review and future research directions, Transp. Res. Part D. Transp. Environ. 140 (2025) 104642.
[29] J. Xu, X. Luo, J. Zhou, D. Liu, Mass-composite activation energies for recycled binder blends, J. Clean. Prod. 449 (2024) 141608, https://doi.org/10.1016/j.jclepro.2024.141608.
[30] X. Luo, B. Birgisson, R.L. Lytton, Kinetics of healing of asphalt mixtures, J. Clean. Prod. 252 (2020) 119790.
[31] X. Luo, F. Gu, R.L. Lytton, Kinetics-based aging prediction of asphalt mixtures using field deflection data, Int. J. Pavement Eng. 20 (2019) 287–297.
[32] H. Li, X. Luo, Y.Q. Zhang, Pseudo Energy-based kinetic characterization of fatigue in asphalt binders, Zhongguo Gonglu Xuebao/China J. Highw. Transp. 33 (2020) 115–124, https://doi.org/10.19721/j.cnki.1001-7372.2020.10.006.
[33] H. Li, X. Luo, Y. Zhang, A kinetics-based model of fatigue crack growth rate in bituminous material, Int. J. Fatigue 148 (2021) 106185.

[34] D. Zhang, B. Birgisson, X. Luo, I. Onifade, A new long-term aging model for asphalt pavements using morphology-kinetics based approach, Constr. Build. Mater. 229 (2019) 117032, https://doi.org/10.1016/j.conbuildmat.2019.117032.
[35] N. Saboo, B. Singh, P. Kumar, Development of high-temperature ranking parameter for asphalt binders using arrhenius model, J. Mater. Civ. Eng. 31 (2019) 4019297.
[36] X. Luo, J. Ling, H. Li, Y. Zhang, Y. Li, Nonlinear viscoelastoplastic kinetics for high-temperature performance of modified asphalt binders, Mech. Mater. 180 (2023) 104612, https://doi.org/10.1016/j.mechmat.2023.104612.
[37] Z. Ding, J. Zhang, P. Li, X. Yue, H. Bing, Analysis of viscous flow properties of styrene–butadiene–styrene-modified asphalt, Constr. Build. Mater. 229 (2019) 116881.
[38] B. Liang, Y. Chen, F. Lan, J. Zheng, Evaluation of rheological and aging behavior of modified asphalt based on activation energy of viscous flow, Constr. Build. Mater. 321 (2022) 126347, https://doi.org/10.1016/j.conbuildmat.2022.126347.
[39] R. Aashto, Standard practice for accelerated aging of asphalt binder using a pressurized aging vessel (PAV), Am. Assoc. State Highw. Transp. Off. (2009).
[40] Z. Ju, D. Ge, H. Zhang, S. Lv, Y. Xue, Rheological behavior and microscopic characteristic of electromagnetic thermal activated crumb rubber and SBS modified asphalt, Constr. Build. Mater. 444 (2024) 137892.
[41] H. Xiao, D. Cao, Z. Qin, H. Yi, X. Chen, Research on the effects of SBS swelling, thermal-oxidative aging, and sulfur crosslinking on chemical composition and rheological properties of SBS-modified asphalt, Int. J. Pavement Res. Technol. (2023) 1–21.
[42] R. Luo, D. Zhang, Z. Zeng, R.L. Lytton, Effect of surface tension on the measurement of surface energy components of asphalt binders using the wilhelmy plate method, Constr. Build. Mater. 98 (2015) 900–909.
[43] P.C. Hiemenz, R. Rajagopalan, Principles of colloid and surface chemistry, revised and expanded, CRC Press, 2016, https://doi.org/10.1201/9781315274287.
[44] H. Li, Y. Zhang, Q. Chen, Z. Xu, X. Luo, Rheological and bonding properties of aged bio-bitumen derived from slow pyrolysis of bamboo waste, Constr. Build. Mater. 438 (2024) 136990, https://doi.org/10.1016/j.conbuildmat.2024.136990.
[45] A.S. for T. and Materials, ASTM D4402-06 Standard Test Method for Viscosity Determination of Asphalt at Elevated Temperatures Using a Rotational Viscometer, in: Annu. B. ASTM Stand., 2006: pp. 1–4.
[46] T. AASHTO, Standard method of test for multiple stress creep recovery (MSCR) test of asphalt binder using a dynamic shear rheometer (DSR), Am. Assoc. State Highw. Transp. Off, Washington, DC, 2009.
[47] P. Chen, J. Wang, X. Luo, L. Wang, Y. Zhang, Multiscale modelling of bitumen-aggregate interfaces from molecular debonding to pull-off strength, Int. J. Adhes. Adhes. 124 (2023) 103393.
[48] J. Wang, S. Cao, X. Luo, Y. Zhang, Characterizing bitumen-aggregate interfacial failures under coupled size effects of bitumen film thickness and aggregate surface roughness, Constr. Build. Mater. 416 (2024) 135238.
[49] M. Fakhri, M.A. Norouzi, Rheological and ageing properties of asphalt bio-binders containing lignin and waste engine oil, Constr. Build. Mater. 321 (2022) 126364.
[50] N. Yalikun, S. Yu, H. Yang, C. Liu, H. Zhang, Q. Wang, Y. Zhang, F. Chen, Preparation and performance study of oxidized CR/SBS composite modified asphalt, J. Environ. Chem. Eng. (2025) 117094.
[51] W. Huang, Y. Li, Y. Meng, C. He, X. Ye, X. Chen, C. Hu, Comprehensive study on the performance of SBS and crumb rubber composite modified asphalt based on the rubber pretreatment technology, Case Stud. Constr. Mater. 20 (2024) e03141, https://doi.org/10.1016/j.cscm.2024.e03141.
[52] A. Eltwati, A. Mohamed, M.R. Hainin, E. Jusli, M. Enieb, Rejuvenation of aged asphalt binders by waste engine oil and SBS blend: physical, chemical, and rheological properties of binders and mechanical evaluations of mixtures, Constr. Build. Mater. 346 (2022) 128441, https://doi.org/10.1016/j.conbuildmat.2022.128441.
[53] X. Luo, F. Gu, R.L. Lytton, Prediction of field aging gradient in asphalt pavements, Transp. Res. Rec. J. Transp. Res. Board 2507 (2015) 19–28, https://doi.org/10.3141/2507-03.
[54] J.C. Petersen, P.M. Harnsberger, Asphalt aging: dual oxidation mechanism and its interrelationships with asphalt composition and oxidative age hardening, Transp. Res. Rec. 1638 (1998) 47–55.
[55] D. Mirzaiyan, M. Ameri, A. Amini, M. Sabouri, A. Norouzi, Evaluation of the performance and temperature susceptibility of gilsonite-and SBS-modified asphalt binders, Constr. Build. Mater. 207 (2019) 679–692.
[56] D. Zhang, B. Birgisson, X. Luo, I. Onifade, A new short-term aging model for asphalt binders based on rheological activation energy, Mater. Struct. 52 (2019) 68.
[57] R.A. Schapery, Correspondence principles and a generalized j integral for large deformation and fracture analysis of viscoelastic media, Int. J. Fract. 25 (1984) 195–223.
[58] L. Luo, Y. Liu, M. Oeser, A.G. Hernandez, P. Liu, Unraveling the nano-cracking mechanism in aged asphalt binder with consideration of rejuvenation effects, Eng. Fract. Mech. 292 (2023) 109683.
[59] H. Bahia, N. Tabatabaee, C. Clopotel, A. Golalipour, Evaluation of the MSCR test for modified binder specification, in: CTAA Annu. Conf. Proceedings-Canadian Tech. Asph. Assoc., 2011: p. 203.
[60] D. Wang, J. Zhu, L. Porot, A. Cannone Falchetto, S. Damen, Multiple stress creep and recovery test for bituminous binders–influence of several key experimental parameters, Road. Mater. Pavement Des. 24 (2023) 290–308.
[61] H. Wang, Y. Huang, K. Jin, Z. Zhou, Properties and mechanism of SBS/crumb rubber composite high viscosity modified asphalt, J. Clean. Prod. 378 (2022) 134534.
[62] W. Zhao, J. Geng, M. Chen, X. Li, Y. Niu, Analysis of SBS content quantitative determination and rheological properties of aged modified asphalt binder, Constr. Build. Mater. 403 (2023) 133024, https://doi.org/10.1016/j.conbuildmat.2023.133024.
[63] P. Li, Z. Ding, L. xia Ma, Z. gang Feng, Analysis of viscous flow properties of asphalt in aging process, Constr. Build. Mater. 124 (2016) 631–638.
[64] S. Liu, L. Shan, C. Qi, W. Zhang, G. Li, B. Wang, W. Wei, Effect of SBS structure on viscosity of SBS-modified asphalt based on molecular dynamics: insights from shearing phase morphology, adsorption and swelling mechanisms, J. Mol. Liq. 393 (2024) 123567.
[65] X. Zheng, W. Xu, H. Xu, S. Wu, K. Cao, Research on the ability of bio-rejuvenators to disaggregate oxidized asphaltene nanoclusters in aged asphalt, ACS Omega 7 (2022) 21736–21749.
[66] P. Saha Chowdhury, R.S. Mullapudi, M.A. Reddy, An investigation on the effect of aging on chemical and mechanical properties of asphalt binders, J. Mater. Civ. Eng. 34 (2022) 4022252.
[67] L. Xu, S. Magar, Z. Zhao, Q. Xiang, F. Xiao, Rheological and anti-moisture characteristics of rubberized reclaimed asphalt pavement with interfacial bond behavior, J. Clean. Prod. 391 (2023) 136172.
[68] Y. Gao, X. Yu, H. Zhang, Q. Xia, P. He, K. Xiao, Mechanisms for improving the adhesion of oil-rich RAP fine aggregate asphalt mortars to aggregates, Constr. Build. Mater. 435 (2024) 136785.
[69] A.S. Mohamed, Z. Cao, X. Xu, F. Xiao, T. Abdel-Wahed, Bonding, rheological, and physiochemical characteristics of reclaimed asphalt rejuvenated by crumb rubber modified binder, J. Clean. Prod. 373 (2022) 133896.
[70] S. Yan, C. Zhou, J. Ouyang, Rejuvenation effect of waste cooking oil on the adhesion characteristics of aged asphalt to aggregates, Constr. Build. Mater. 327 (2022) 126907.
[71] S. Abbas, S.B.A. Zaidi, I. Ahmed, Performance evaluation of asphalt binders modified with waste engine oil and various additives, Int. J. Pavement Eng. 24 (2023) 2128353.